# Electronic Supplementary Information

Frontier orbital engineering of

photo-hydrogen-evolving molecular devices:

a clear relationship between the H₂-evolving activity

and the energy level of the LUMO

Shigeyuki Masaoka,[a,b] Yuichiro Mukawa,[a] and Ken Sakai[*a]

[a]*Department of Chemistry, Faculty of Science, Kyushu University, Hakozaki 6-10-1,*

Higashi-ku, Fukuoka 812-8581, Japan. [b]*PRESTO, Japan Science and Technology*

*Agency (JST), Honcho 4-1-8, Kawaguchi, Saitama, 332-0012, Japan.*

Absorption spectra
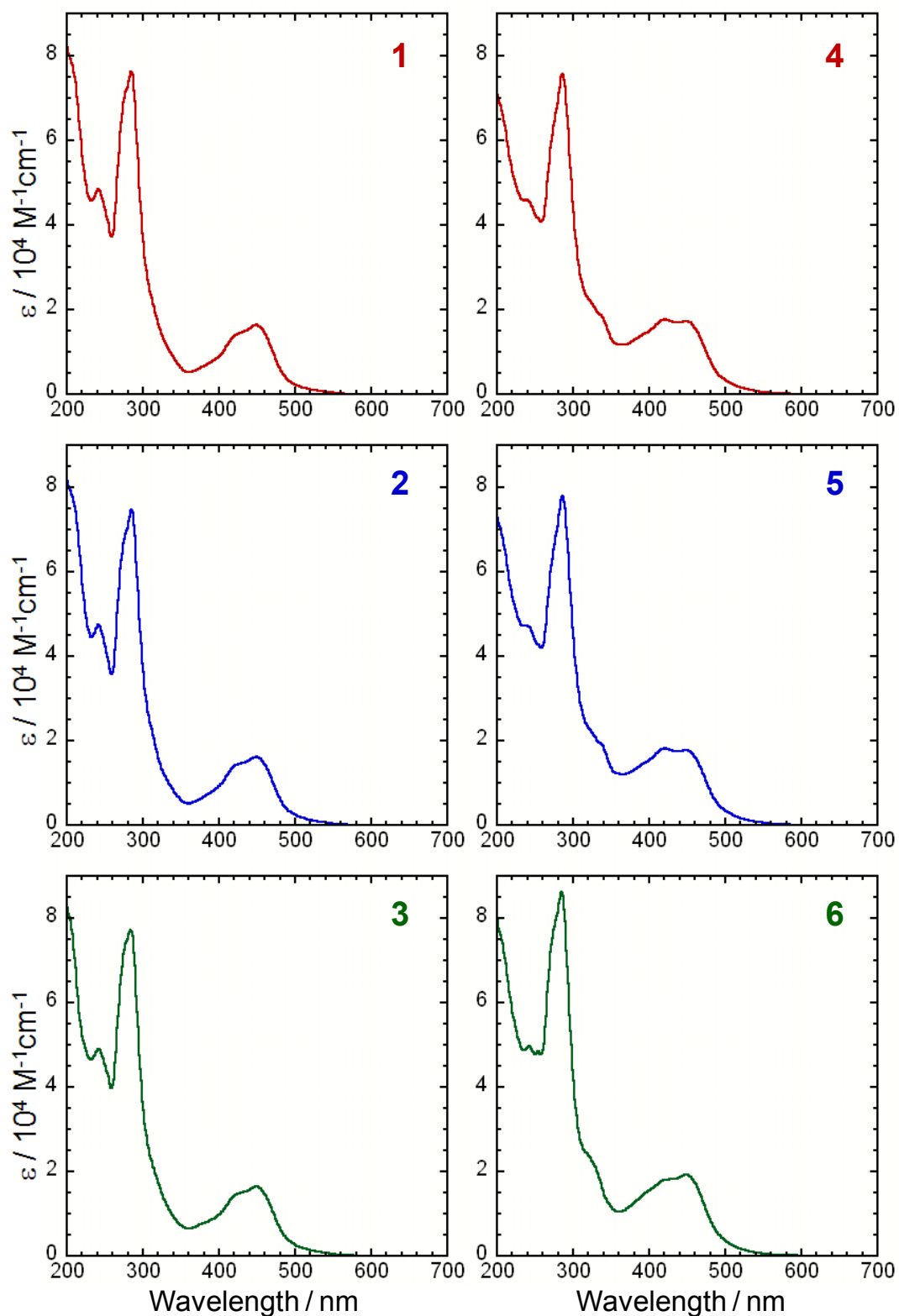
Figure S1. Absorption spectra of [**1**](PF$_6$)$_2$·H$_2$O, [**2**](PF$_6$)$_2$·1.5H$_2$O, [**3**](PF$_6$)$_2$·5H$_2$O, [**4**](PF$_6$)$_2$·H$_2$O, [**5**](PF$_6$)$_2$·3H$_2$O and [**6**](PF$_6$)$_2$·3H$_2$O in acetonitrile at 20 °C in air.

Emission spectra
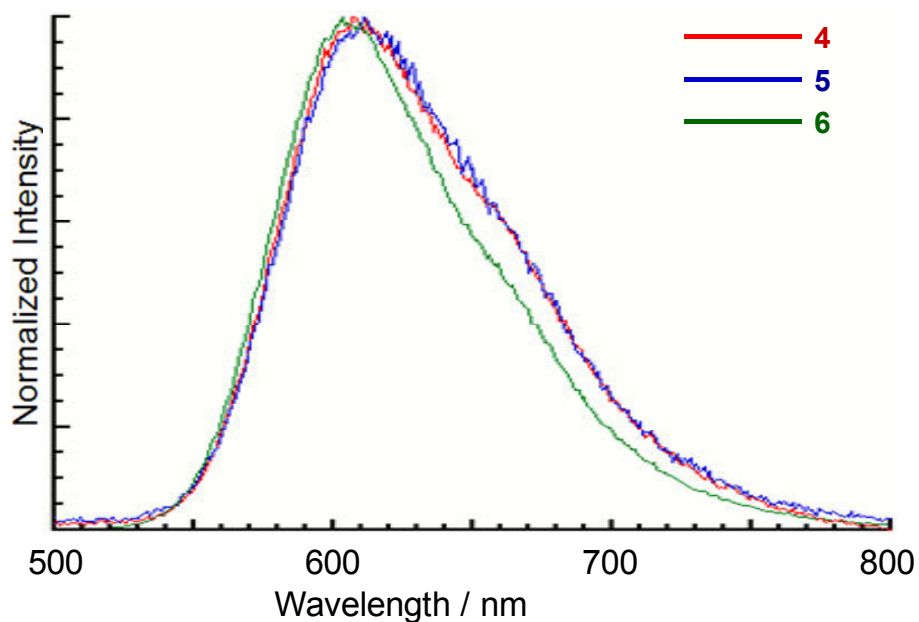
Figure S2. Normalized emission spectra of [**4**]$(PF_6)_2 \cdot H_2O$ (red), [**5**]$(PF_6)_2 \cdot 3H_2O$ (blue) and [**6**]$(PF_6)_2 \cdot 3H_2O$ (green) in acetonitrile at 25 °C under degassed condition. The spectra were not corrected for the overall sensitivity of the detector.

Electrochemistry
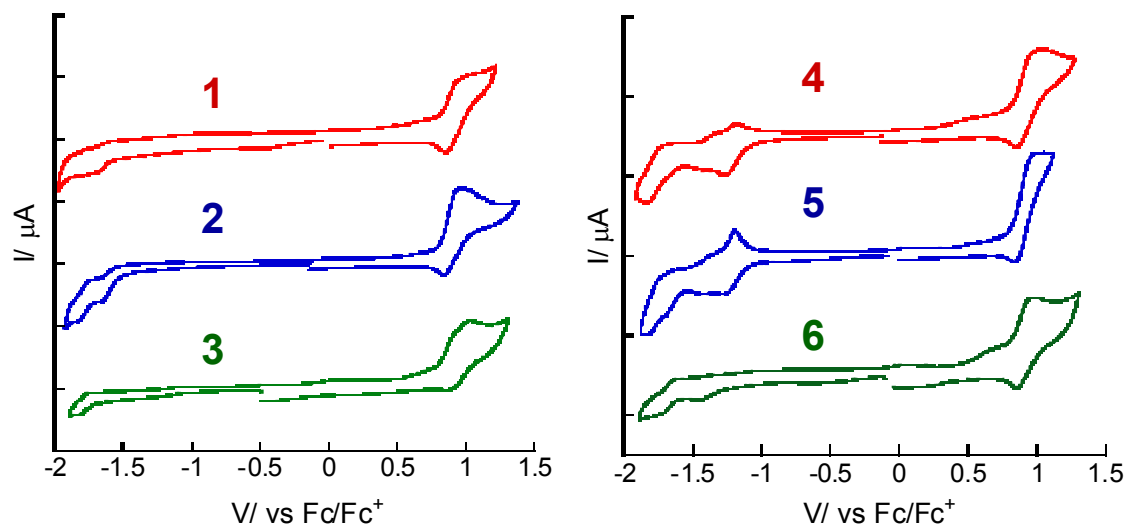
Figure S3a. Left: Cyclic voltammograms of [**1**]$(PF_6)_2 \cdot H_2O$ (red), [**2**]$(PF_6)_2 \cdot 1.5H_2O$ (blue) and [**3**]$(PF_6)_2 \cdot 5H_2O$ (green) in 0.1 M TBAP/dry acetonitrile, recorded at a scan rate of 50 mVs^{-1}. Right: Cyclic voltammograms of [**4**]$(PF_6)_2 \cdot H_2O$ (red), [**5**]$(PF_6)_2 \cdot 3H_2O$ (blue) and [**6**]$(PF_6)_2 \cdot 3H_2O$ (green) in 0.1 M TBAP/dry acetonitrile, recorded at a scan rate of 50 mVs^{-1}.
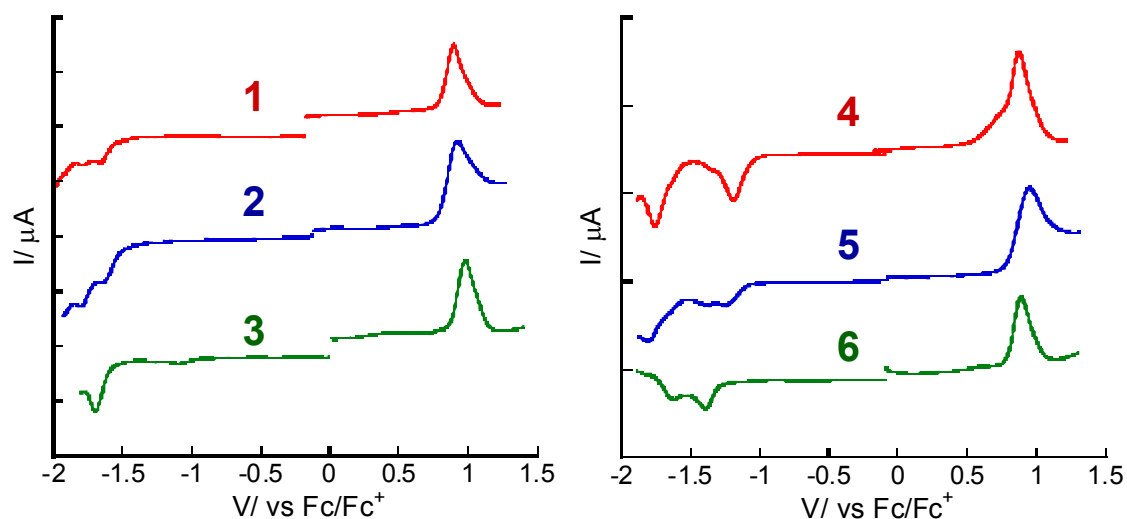
Figure S3b. Left: Square-wave voltammograms of [**1**]$(PF_6)_2 \cdot H_2O$ (red), [**2**]$(PF_6)_2 \cdot 1.5H_2O$ (blue) and [**3**]$(PF_6)_2 \cdot 5H_2O$ (green) in 0.1 M TBAP/dry acetonitrile, recorded at a step potential of 4 mV, an amplitude of 25 mV, and a frequency of 15 Hz. Right: Square-wave voltammograms of [**4**]$(PF_6)_2 \cdot H_2O$ (red), [**5**]$(PF_6)_2 \cdot 3H_2O$ (blue) and [**6**]$(PF_6)_2 \cdot 3H_2O$ (green) in 0.1 M TBAP/dry acetonitrile, recorded at a step potential of 4 mV, an amplitude of 25 mV, and a frequency of 15 Hz.

DFT calculation
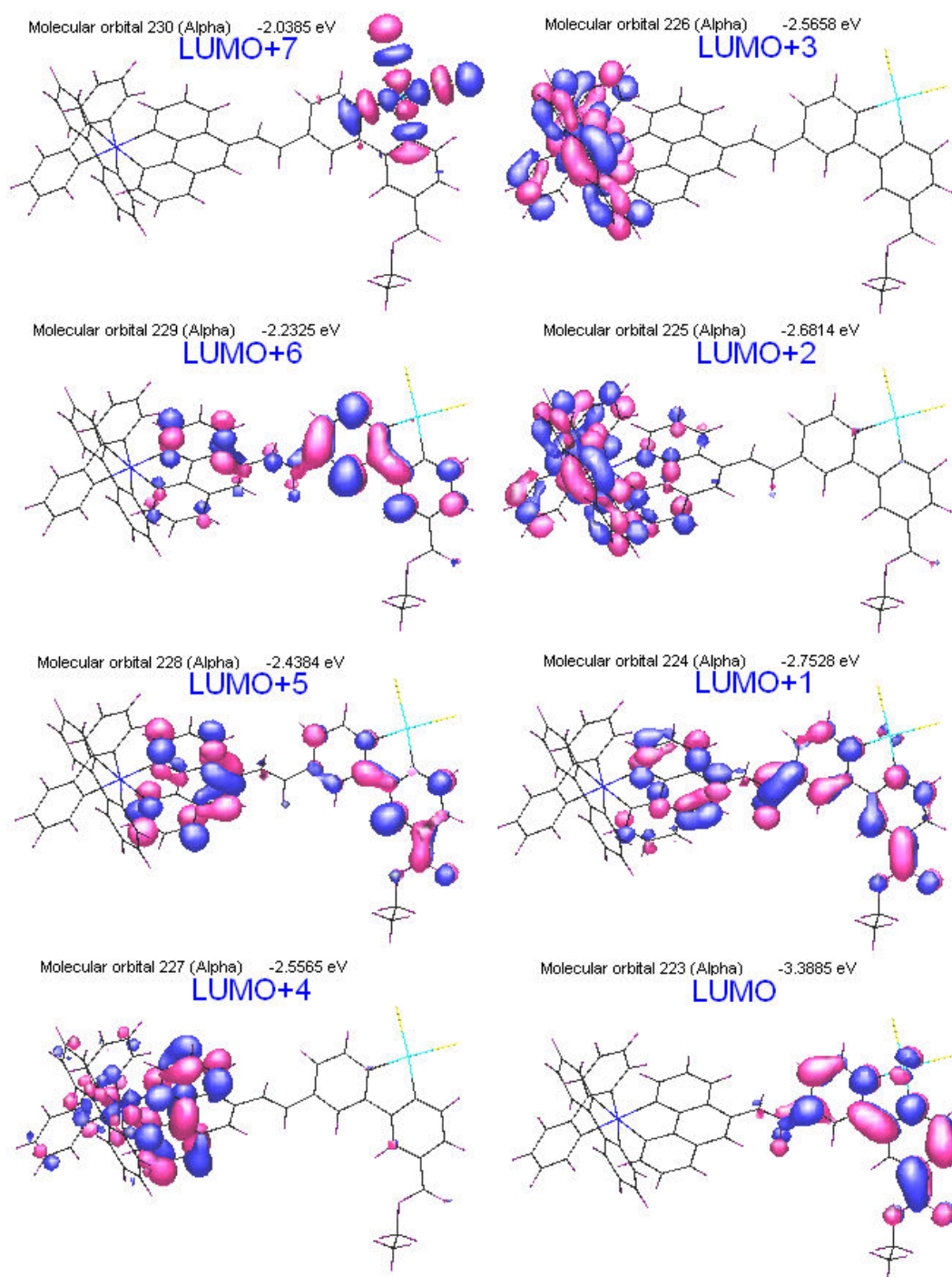
Figure S4a. Frontier molecular orbitals of a fully optimized structure of [**5**]$^{2+}$ in water (polarizable continuum model), obtained by using the B3LYP level of DFT and the LanL2DZ basis set implemented in the Gaussian 03 suite programs.
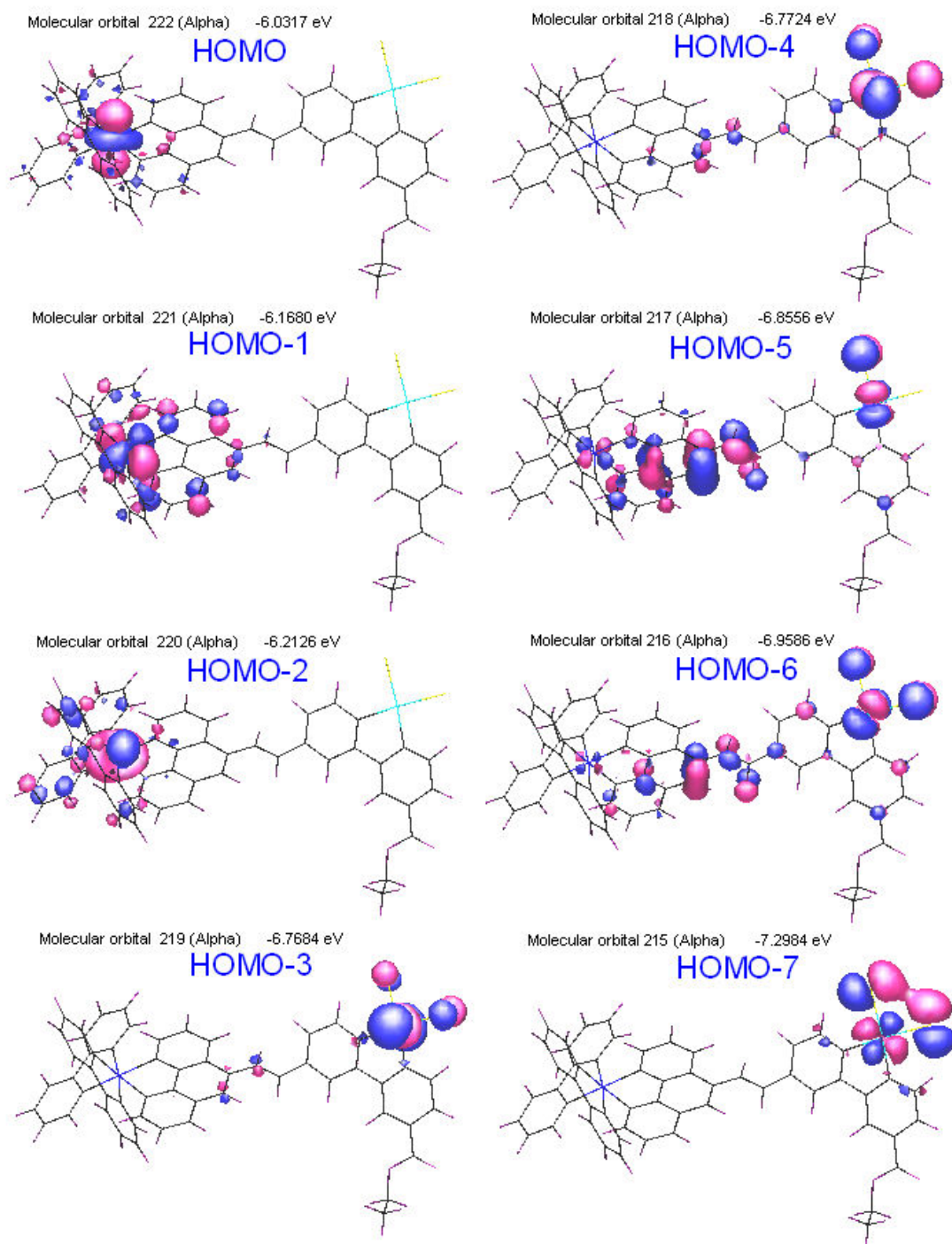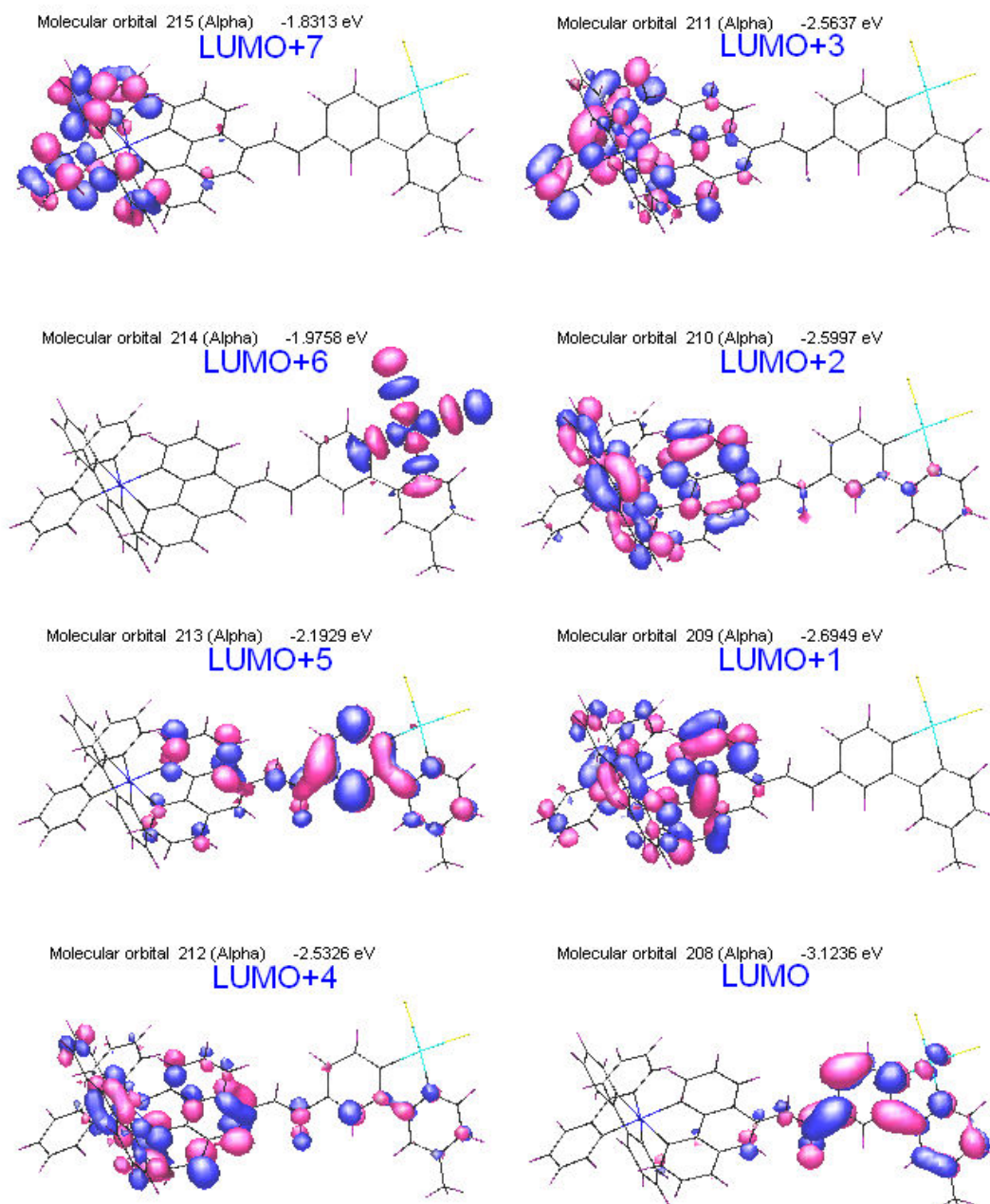
Figure S4b. Frontier molecular orbitals of a fully optimized structure of [**5**]$^{2+}$ in water (polarizable continuum model), obtained by using the B3LYP level of DFT and the LanL2DZ basis set implemented in the Gaussian 03 suite programs.

Molecular orbital 215 (Alpha)   -1.8313 eV
LUMO+7

Molecular orbital 211 (Alpha)   -2.5637 eV
LUMO+3

Molecular orbital 214 (Alpha)   -1.9758 eV
LUMO+6

Molecular orbital 210 (Alpha)   -2.5997 eV
LUMO+2

Molecular orbital 213 (Alpha)   -2.1929 eV
LUMO+5

Molecular orbital 209 (Alpha)   -2.6949 eV
LUMO+1

Molecular orbital 212 (Alpha)   -2.5326 eV
LUMO+4

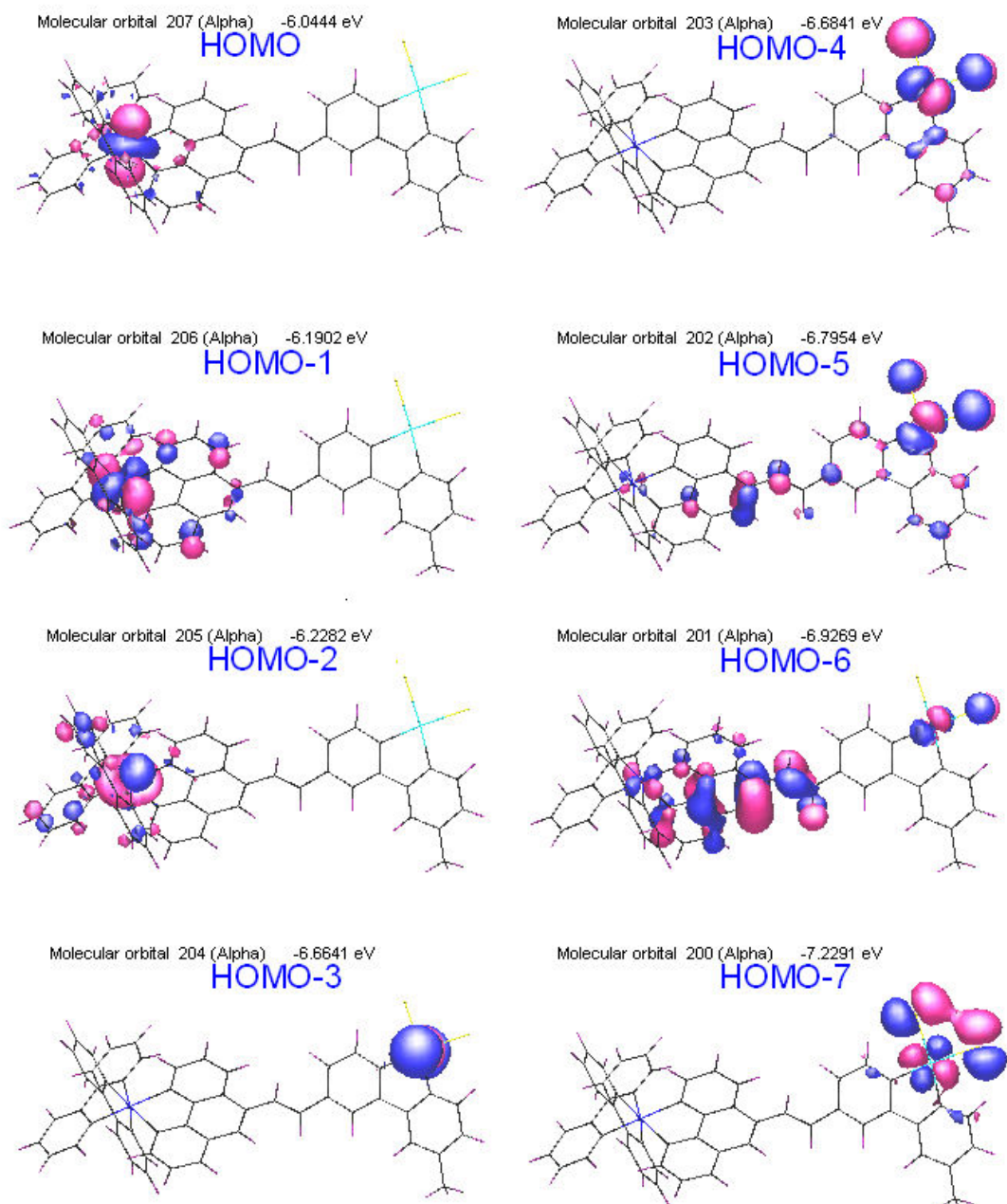Molecular orbital 208 (Alpha)   -3.1236 eV
LUMO

Figure S5a. Frontier molecular orbitals of a fully optimized structure of [**6**]$^{2+}$ in water (polarizable continuum model), obtained by using the B3LYP level of DFT and the LanL2DZ basis set implemented in the Gaussian 03 suite programs.

Molecular orbital 207 (Alpha)   -6.0444 eV
HOMO

Molecular orbital 203 (Alpha)   -6.6841 eV
HOMO-4

Molecular orbital 206 (Alpha)   -6.1902 eV
HOMO-1

Molecular orbital 202 (Alpha)   -6.7954 eV
HOMO-5

Molecular orbital 205 (Alpha)   -6.2282 eV
HOMO-2

Molecular orbital 201 (Alpha)   -6.9269 eV
HOMO-6

Molecular orbital 204 (Alpha)   -6.6641 eV
HOMO-3

Molecular orbital 200 (Alpha)   -7.2291 eV
HOMO-7

Figure S5b. Frontier molecular orbitals of a fully optimized structure of [**6**]$^{2+}$ in water (polarizable continuum model), obtained by using the B3LYP level of DFT and the LanL2DZ basis set implemented in the Gaussian 03 suite programs.
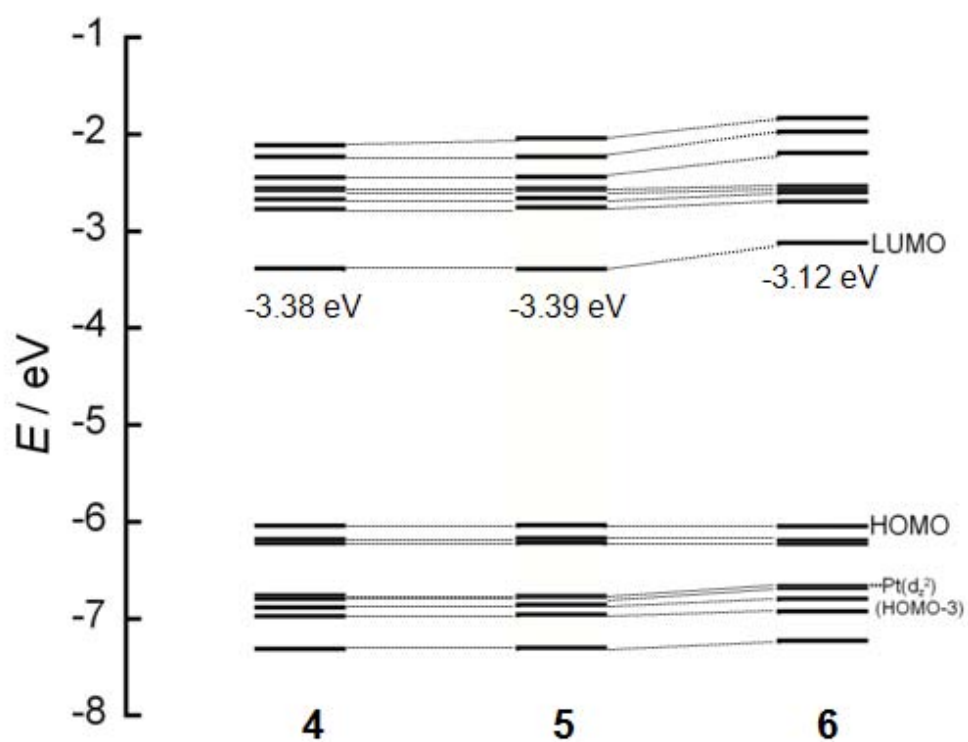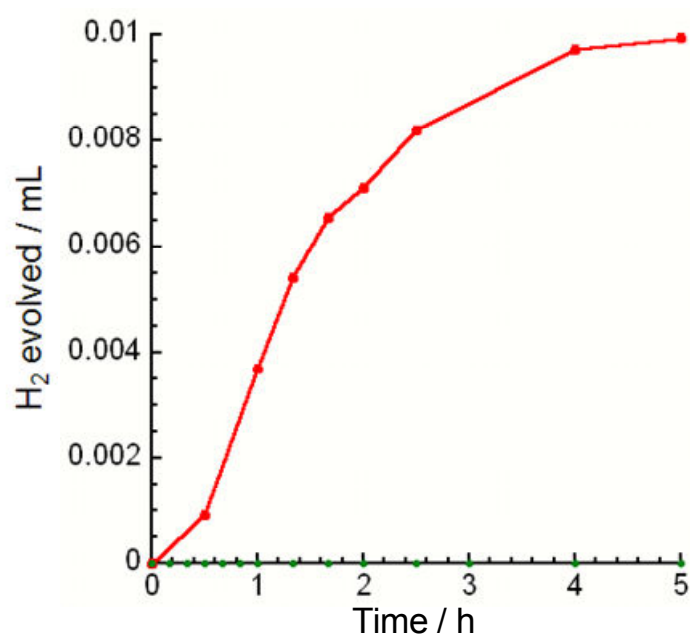
Figure S6. MO energy diagrams for the Ru(II)Pt(II) dimers, **4-6**, obtained by the DFT calculations.

Photochemical hydrogen production form water

Figure S7. Photochemical H_2 production from an aqueous acetate buffer solution (0.03 M CH_3CO_2H and 0.07 M CH_3CO_2Na; pH 5.0, 10 mL) containing 30 mM EDTA, and 0.1 mM [**6**]$(NO_3)_2\cdot2H_2O$ in the absence (green) and presence of 2.0 mM $MV(NO_3)_2$ (red).

Emission decay profiles
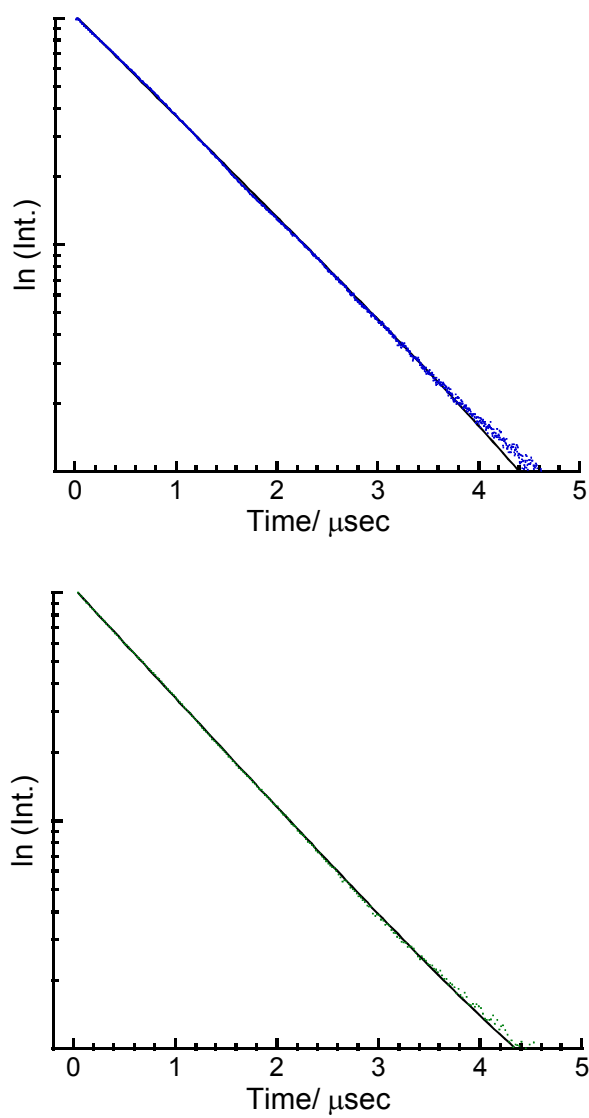
Figure S8. Emission decay profiles of [**2**](PF$_6$)$_2$·1.5H$_2$O (top) and [**3**](PF$_6$)$_2$·5H$_2$O (bottom) in acetonitrile at 25 °C under degassed condition. Colored dots correspond to the observed data and solid lines denote calculated lines according to a monoexponential functions (τ = 957 and 901 ns for **2** and **3**, respectively).

Nanosecond transient absorption spectra
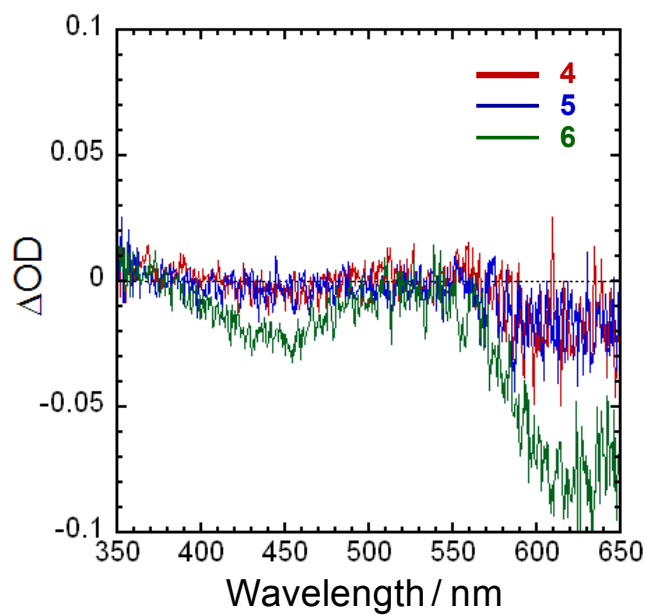
Figure S9. Transient absorption spectra of [**4**](PF$_6$)$_2$·H$_2$O (red), [**5**](PF$_6$)$_2$·3H$_2$O (blue) and [**6**](PF$_6$)$_2$·3H$_2$O (green) at 10 ns after laser pulse excitation at λ = 266 nm in water at 20 °C under degassed condition.